Fabrication of SiC nanowire thin-film transistors using dielectrophoresis*

Dai Zhenqing(戴振清)[1,2], Zhang Liying(张丽英)[1], Chen Changxin(陈长鑫)[1], Qian Bingjian(钱炳建)[1], Xu Dong(徐东)[1], Chen Haiyan(陈海燕)[1], Wei Liangming(魏良明)[1], and Zhang Yafei(张亚非)[1,†]

[1]Key Laboratory for Thin Film and Microfabrication of the Ministry of Education, Research Institute of Micro and Nano Science and Technology, Shanghai Jiao Tong University, Shanghai 200240, China
[2]Department of Physics and Chemistry, Hebei Normal University of Science and Technology, Qinhuangdao 066004, China

Abstract: The selection of solvents for SiC nanowires (NWs) in a dielectrophoretic process is discussed theoretically and experimentally. From the viewpoints of dielectrophoresis force and torque, volatility, as well as toxicity, isopropanol (IPA) is considered as a proper candidate. By using the dielectrophoretic process, SiC NWs are aligned and NW thin films are prepared. The densities of the aligned SiC NWs are 2 μm^{-1}, 4 μm^{-1}, 6 μm^{-1}, which corresponds to SiC NW concentrations of 0.1 $\mu g/\mu L$, 0.3 $\mu g/\mu L$ and 0.5 $\mu g/\mu L$, respectively. Thin-film transistors are fabricated based on the aligned SiC NWs of 6 μm^{-1}. The mobility of a typical device is estimated to be 13.4 $cm^2/(V{\cdot}s)$.

Key words: dielectrophoresis; SiC nanowires; thin-film transistors
DOI: 10.1088/1674-4926/33/11/114001 **EEACC:** 2550

1. Introduction

One-dimensional nanomaterials have many outstanding characteristics compared with their corresponding bulk ones. Fabrication of electron devices is one of their important applications[1−4]. The wide band-gap material SiC has many superior properties, such as high critical breakdown field strength (2×10^6 V/cm), high thermal conductivity (4.9 W/(K·cm)), high saturated drift velocity (2×10^7 cm/s), as well as excellent physical and chemical stability, which make it be a good material for fabricating high temperature and high power devices[5−8]. The combination of the distinctive properties of SiC with one-dimensional structures, such as field-effect transistors based on SiCNWs (SiC NWFETs), may provide excellent candidates for high temperature and high power applications.

So far, a few studies on SiC NWFETs have been reported[9−14]. The highly n-type doped SiC NWs used to prepare NWFETs led to a weak gate-effect[9]. The on/off current ratio of the SiC NWFETs was $\sim 10^3$ when the contacts between Au and SiC NWs were Schottky contacts[10]. A theoretical study has shown that SiC NWFETs had similar performance to the Si-based ones while they will offer all advantages from the SiC physical properties for high temperature and high power applications[11]. In addition, high densities of interface trap states and fixed charge have degraded the performance of SiC NWFETs[12]. The specific contact resistance values of Ni/Au ohmic contacts on SiC NWs were $\sim$ 40 times lower than those of Ti/Au ohmic contacts[13]. The latest study has shown that various shapes of drain current versus the drain–source voltage curves (linear, nonlinear symmetric, and asymmetric) of SiC NWFETs were observed on the same substrate, an origin for which was might be a non-uniformity in annealing, NW doping level and high interface traps density as well as the high sensitivity of the metal-NW contacts to local surface contaminations[14].

The prepared SiC NWFETs use single NWs[9−14]. A single SiC NW cannot carry large current, so NWFETs based on it are difficult to use at high power. In addition, SiC NWs may be damaged in extreme conditions, which easily leads to the failure of FETs based on a single SiC NW. Thin films of NWs enable high current outputs[15−17]. Moreover, even if several NWs were damaged, SiC NWFETs could also work well. In addition, a difference of diameter of NWs is evident[18,19], which leads to device-to-device variety because of the diameter determining the properties of NWs to some extent[20,21]. A thin film of NWs may overcome the problem in that it provides good device-to-device uniformity with statistical averaging effects[15,16,22,23]. Thin films consist of random networks or well-aligned arrays of SiC NWs, and the aligned arrays have advantages compared with the random networks[17,24]. Several schemes have been proposed to manipulate and align one dimensional nanostructures, including CVD[15], Langmuir–Blodgett[25], microfluidic [26], and dielectrophoresis[27−35]. Among them, dielectrophoresis is one of the most effective techniques used to construct various electronic devices[27−32].

Choice of solvent is an important issue for the dielectrophoresis process. Ethanol[32,36−38], IPA[31,39−41], highly purified water[29,30,31,42], and dimethyl formamide (DMF)[32,43,44] are usually used as a solvent for one dimensional nanostructures in dielectrophoresis, and it is necessary to determine which one among them is a proper solvent for SiC.

In this paper, we discuss the selection of solvents for

* Project supported by the National Natural Science Foundation of China (Nos. 50730008, 60807008) and the Doctoral Fund of Hebei Normal University of Science and Technology, China (No. 2009YB007).
† Corresponding author. Email: yfzhang@sjtu.edu.cn
Received 29 April 2012, revised manuscript received 10 June 2012

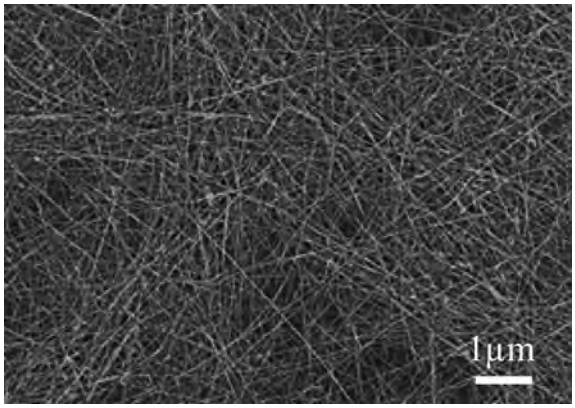

Fig. 1. SEM image of the synthesized SiC NWs.

SiC NWs in the dielectrophoretic process. Directed SiC NWs are obtained using dielectrophoresis, and thin films based on aligned SiC NWs are prepared. The present process of aligning SiC NWs has advantages in simple setup and easy operation. NWTFTs are prepared based on thin films of aligned SiC NWs, and their electrical properties are measured on an Agilent 4156C semiconductor parameter analyzer.

2. Experimental

The β-SiC NWs were synthesized by using a carbon thermal reduction method without the use of a metal catalyst. SiO powders were heated by high-frequency induction sources, and then the formed SiO gas was carried to an activated carbon fiber surface. The reactions between the SiO and the activated carbon fiber led to the formation of β-SiC NWs[45]. An SEM image of the synthesized SiC NWs is shown in Fig. 1. The length of the synthesized SiC NWs is up to 10 μm, and their average diameter is about 20 nm. It was found that the as-synthesized SiC NWs were coated by a SiO_2 layer. In order to improve the contacts between metal electrodes and SiC NWs, the SiC NWs were dipped into 5% HF and then centrifuged several times (18000 rpm and 30 min for every time) to remove HF completely. Finally, the as-treated SiC NWs were dipped into ethanol, highly purified water, DMF, and IPA, respectively, and then ultrasonically treated for 3 h in order to obtain uniform and stable suspension. The suspension was left for 30 min before it was used for dielectrophoresis.

Using standard lithography and the lift-off technique, parallel source and drain electrodes (Au, 200 nm) were patterned on heavily doped n-type silicon wafers with a 400-nm-thick SiO_2 layer. The electrodes have a length of 100 μm, and a gap of 1.4 μm or 5.0 μm. For an electrode with a gap of 1.4 μm, a drop of ethanol suspension of SiC NWs ($\sim$ 0.5 μL, the SiC NW concentration is 0.3 μg/μL) was introduced onto the gap of the electrode, and a 7 V AC bias with a frequency of 1 MHz was applied between the source and drain electrode. The AC bias was switched off after the ethanol solvent was evaporated. Ethanol was replaced by highly purified water, DMF and IPA in turn as the solvents for SiC NWs to carry out dielectrophoresis. For an electrode with a gap of 5.0 μm, only IPA was selected as the solvent for the SiC NWs and a 50 V AC bias with a frequency of 1 MHz was applied to carry out dielectrophoresis. Finally, the wafer containing SiC NWs was heat-treated for 30 s at 550 ℃ in N_2 flow to improve the contact between NWs and Au electrodes.

3. Result and discussion

3.1. Alignment of SiC NWs

3.1.1. Choice of solvents

The phenomenon of dielectrophoresis was explained by the theory of effective dipole moment. When a drop of SiC NWs suspension is introduced onto the gap of the electrodes applied with an AC electric field, the SiC NWS are polarized by the electric field. Effective dipole moments are induced by the polarization process. The induced torque and force on such an effective dipole are expressed as[36]

$$\langle T\rangle = \frac{1}{2}\pi r^2 l E^2 \varepsilon_{\rm m} \sin\theta\cos\theta\ {\rm Re}\left[\frac{(\tilde{\varepsilon}_{\rm NW}-\tilde{\varepsilon}_{\rm m})^2}{\tilde{\varepsilon}_{\rm m}\,(\tilde{\varepsilon}_{\rm NW}+\tilde{\varepsilon}_{\rm m})}\right], \quad (1)$$

$$\boldsymbol{F}_{\rm DEP} = \frac{1}{2}\pi r^2 l \varepsilon_{\rm m}{\rm Re}\left(\frac{\tilde{\varepsilon}_{\rm NW}-\tilde{\varepsilon}_{\rm m}}{\tilde{\varepsilon}_{\rm m}}\right)\nabla E^2, \quad (2)$$

where r and l are the radius and length of SiC NWs, respectively, E is the root mean square value of the electric field strength, $\varepsilon_{\rm m}$ is the real permittivity of the suspending medium, ${\rm Re}\{(\tilde{\varepsilon}_{\rm NW}-\tilde{\varepsilon}_{\rm m})^2/[\tilde{\varepsilon}_{\rm m}\,(\tilde{\varepsilon}_{\rm NW}+\tilde{\varepsilon}_{\rm m})]\}$ and ${\rm Re}[(\tilde{\varepsilon}_{\rm NW}-\tilde{\varepsilon}_{\rm m})/\tilde{\varepsilon}_{\rm m}]$ are the real part of the $(\tilde{\varepsilon}_{\rm NW}-\tilde{\varepsilon}_{\rm m})^2/[\tilde{\varepsilon}_{\rm m}\,(\tilde{\varepsilon}_{\rm NW}+\tilde{\varepsilon}_{\rm m})]$ and $(\tilde{\varepsilon}_{\rm NW}-\tilde{\varepsilon}_{\rm m})/\tilde{\varepsilon}_{\rm m}$, respectively, $\tilde{\varepsilon}_{\rm NW}$ and $\tilde{\varepsilon}_{\rm m}$ are the complex dielectric permittivity of SiC NWs and the suspending medium, which is given by

$$\tilde{\varepsilon} = \varepsilon - i\frac{\sigma}{\omega}, \quad (3)$$

where ε is the real permittivity, σ is the conductivity, and ω is the angular frequency.

The force leads to a translation of SiC NWs towards the maximum or minimum electric field strength, while the torque leads to a rotation of SiC NWs towards the electric field.

The real permittivity of bulk SiC is $9.7\varepsilon_0$ (ε_0 is permittivity of vacuum)[46], which is used as the real permittivity of SiC NWs in this paper. The conductivity of SiC changes with doping concentration[47].

The real permittivities and conductivities of the usually used solvents for a one dimensional nanostructure in dielectrophoresis, such as ethanol, IPA, highly purified water and dimethyl formamide (DMF) are shown in Table 1. If the four substances are respectively used as solvents for SiC NWs, the dielectrophoretic torque and force are calculated with Eqs. (1) and (2) under the condition of an electric field frequency of 1 MHz. In order to simplify calculation, $\varepsilon_{\rm m}{\rm Re}\{(\tilde{\varepsilon}_{\rm NW}-\tilde{\varepsilon}_{\rm m})^2/(\tilde{\varepsilon}_{\rm m}\,[\tilde{\varepsilon}_{\rm NW}+\tilde{\varepsilon}_{\rm m})]\}$ is used as the torque, and $\varepsilon_{\rm m}{\rm Re}\,[(\tilde{\varepsilon}_{\rm NW}-\tilde{\varepsilon}_{\rm m})/\tilde{\varepsilon}_{\rm m}]$ is used as the force. Figure 2(a) shows the torque versus conductivity of the SiC NWs curves, and Figure 2(b) shows the force versus conductivity of the SiC NWs curves. From Fig. 2(a), we come to a conclusion that the torques have little difference on the four solvents. Figure 2(b) shows that the values of the forces are positive. The positive value means that $\boldsymbol{F}_{\rm DEP}$ points to the maximum electric field strength, which leads to SiC NWs being attracted to the electrode edges. In addition, the difference of the forces is evident.

Table 1. Conductivity and relative permittivity of ethanol, IPA, highly purified water, and DMF.

Parameter	Ethanol[36]	IPA[40]	Highly purified water[48]	DMF
Conductivity (S/m)	1.345×10^{-7}	6×10^{-6}	5.5×10^{-6}	3.43×10^{-5}[49]
Relative permittivity	25.3	18.3	77.75	38.25[48]

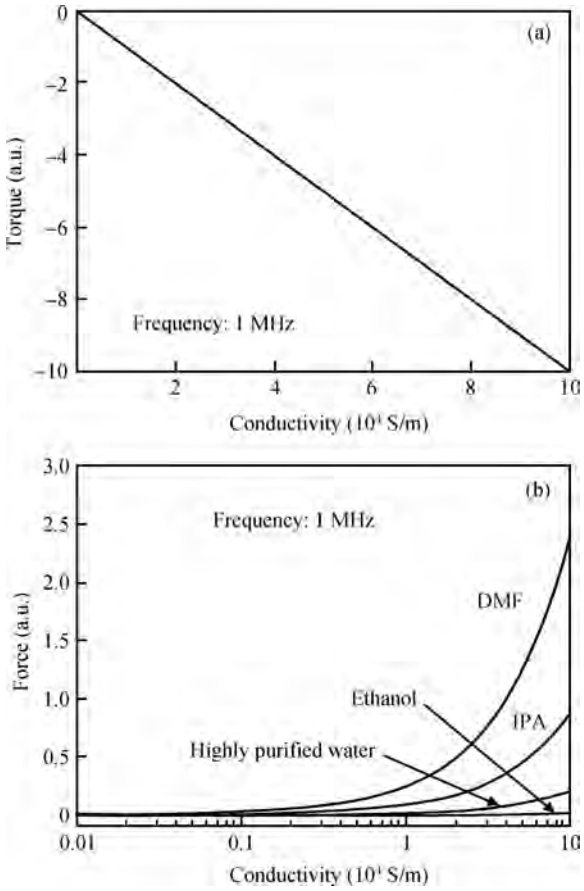

Fig. 2. (a) The dielectrophoretic torque and (b) force versus the conductivity of SiC NW curves.

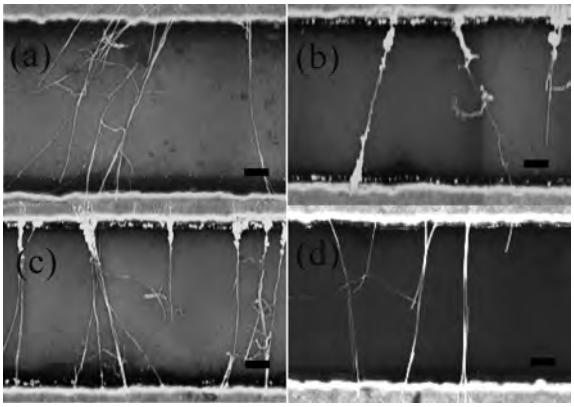

Fig. 3. SEM images of aligned SiC nanowires using dielectrophoresis with (a) ethanol, (b) highly purified water, (c) DMF, and (d) IPA, scale bar 200 nm.

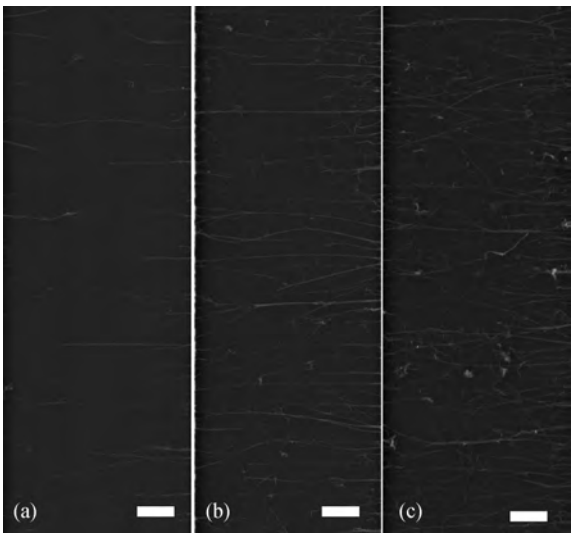

Fig. 4. SEM images of aligned SiC nanowires using dielectrophoresis with IPA, scale bar 1 μm.

The maximum force is induced by DMF, and the second one is induced by IPA. Volatilization of DMF is very slow, and nearly 10 min is need for a drop of 0.5 μL to volatilize completely. The time for aligning a one dimensional nanostructure is $\sim$30 s[41], so it is inefficient that DMF is used as solvent for SiC NWs in the process of dielectrophoresis. However, IPA volatilizes fast, and nearly 45 s is needed for a 0.5 μL drop to volatilize completely. Moreover, the toxicity of IPA is less than that of DMF. The influence of the viscous force is insignificant compared with that of dielectrophoretic force[41] so it is neglected here. Figure 3 shows SEM images of aligned SiC NWs using dielectrophoresis with the above mentioned four different solvents. The SEM images demonstrate that experimental results are consistent with theory. In addition, it can be observed that the SiC NWs are partially covered by nanoparticles with highly purified water and DMF being used in the dielectrophoretic process, but no obvious nanoparticles are observed when ethanol or IPA is used. This is due to the low volatile speed of highly purified water and DMF, which leads to the nanoparticles having enough time to reach the NWs. Therefore, IPA is selected as a solvent for SiC NWs in this paper.

3.1.2. Alignment of SiC NWs

Dielectrophoresis is carried out with different concentrations of IPA suspension of SiC NWs, and the result of dielectrophoresis is shown in Figs. 4(a), 4(b) and 4(c), corresponding to concentrations of 0.1, 0.3, and 0.5 μg/μL, respectively. Density of SiC NWs are $\sim$2, $\sim$4, and $\sim$6 μm^{-1} corresponding to Figs. 4(a), 4(b), and 4(c), respectively, which shows that the density increases with the concentration of SiC NWs suspension rising. In addition, the order of the SiC NWs becomes weak with the concentration of IPA suspension of SiC NWs rising, the reason for which is that the interaction effects between

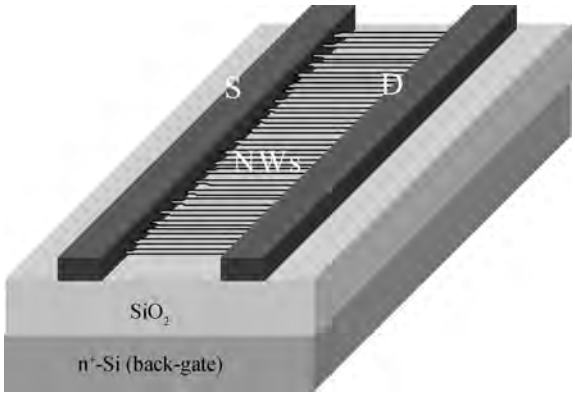

Fig. 5. Schematic view of SiC NWTFTs.

SiC NWs increase when the concentration of SiC NWs suspension increases. From the process of dielectrophoresis, we have to draw a conclusion that the method of aligning SiC NWs has advantages in simple setup and easy operation comparing with others[25−32].

3.2. SiC NWTFTs

A typical SiC NWTFT is prepared with the thin film of aligned SiC NWs of Fig. 4(c). The SiC NWTFT configuration was shown in Fig. 5 where S and D mean source and drain electrodes, respectively. The Si substrate was used as a back gate. The drain current I_D versus the source–drain voltage V_{DS} and the gate voltage V_G are measured. Figure 6(a) shows I_D versus V_{DS} characteristic curves of the SiC NWTFT at different V_G, and Figure 6(b) shows I_D as a function of V_G at different V_{DS}. Figure 6(a) shows that contacts between Au and SiC NWs are Schottky contacts, which is in agreement with a previous report[10]. Figure 6(b) indicates that the SiC NWTFT has the following characteristics: (1) the SiC NWs are n-type semiconductors; (2) the SiC NWTFT has a weak gate-effect, which is similar to previous reports[9, 12, 13]. The weak gate-effect indicates a high carrier concentration. This high n-type character of SiC NWs is attributed to the high density of donor states resulting from N_2 entering into the reactor unintentionally and stacking faults[12]. In addition, the thick SiO_2 layer is another reason for the weak gate-effect. The gate-effect reported in this paper is a little better than that in the reports[9, 12, 13], for which a possible reason is that contacts between electrodes and SiC NWs are Schottky contacts, as compared with the ohmic contacts reported in other papers[9, 10, 12, 13]. The on/off current ratio is estimated to be ∼20 at a V_{DS} of 4 V, in which I_{DS} at a V_G of −20 V is roughly regard as a minimum at the depletion region. The threshold voltage for the device is estimated to be –19.5 V.

The electron field-effect mobility of the SiC NWTFTs is estimated using the equation[50]

$$\mu_{fe} = \frac{g_m}{C_g}\frac{L^2}{V_{DS}}, \tag{4}$$

where $g_m = dI_{ds}/dV_G$ is the linear-region transconductance (g_m is estimated to be 9.2×10^{-6} A/V at a V_{DS} of 4 V), and $L = 5\ \mu$m is the NWTFT channel length. C_g is the total gate capacitance of the NWTFT, which can be estimated by the equation

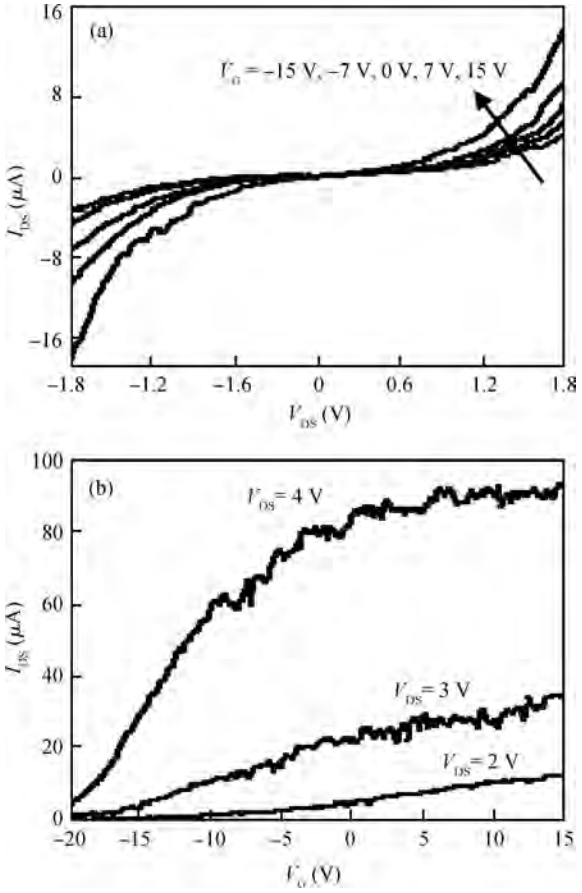

Fig. 6. (a) The drain current I_{DS} versus the drain–source voltage V_{DS} curves of SiC NWFETs at different gate voltages and (b) the drain current I_{DS} versus the gate voltage V_G curves of SiC NWTFT at different drain–source voltages V_{DS}.

$$C_g = C_0(WL), \tag{5}$$

where $W = 100\ \mu$m is the device width, C_0 is the capacitance per unit area. C_0 can be calculated using a parallel plate model, by which the introduced error is less than 5%[15]. With the parallel plate model, C_0 is given as

$$C_0 = \varepsilon_{SiO_2}/d, \tag{6}$$

where $\varepsilon_{SiO_2} = 3.9\varepsilon_0$ is the real permittivity of SiO_2, and $d =$ 400 nm is the thickness of SiO_2. C_0 is estimated to be 8.63×10^{-5} F, and then C_g is estimated to be 4.31×10^{-14} F. So the electron field-effect mobility is estimated to be 13.4 $cm^2/(V{\cdot}s)$. This estimated mobility is low compared with that of bulk SiC, which is attributed to lots of fixed charge and interface trapped charge at the SiC NWs/SiO_2 interface[12].

4. Conclusion

The SiC NWs thin films were obtained by using a dielectrophoresis method. It was found that the density of aligned SiC NWs increased with the concentration of SiC NW suspension rising. The interaction effects of SiC NWs increase in highly concentrated SiC NWs suspensions, which is responsible for the order getting weak. From the viewpoints of dielectrophoresis force and torque, volatility, as well as toxicity,

IPA is a proper solvent for SiC NWS. The TFT based on a thin film of aligned SiC NWs has a weak gate-effect, for which the high n-type character of SiC NWs and thick SiO_2 layer are responsible. The on/off current ratio of the TFT is ~ 20 at a V_{DS} of 4 V, and the threshold voltage is estimate to be –19.5 V for the device. The electron field-effect mobility is 13.4 $cm^2/(V{\cdot}s)$, and lots of fixed charge and interface trapped charge at SiC NWs/SiO_2 interface lead to the low mobility.

References

[1] Avouris P, Chen Z H, Perebeinos V. Carbon-based electronics. Nature Nanotechnology, 2007, 2: 605

[2] Xia Y N, Yang P D, Sun Y G. One-dimensional nanostructures: synthesis, characterization, and applications. Adv Mater, 2003, 15: 353

[3] Fu X J, Zhang H Y, Guo C X, et al. Fabrication and photoelectrical characteristics of ZnO nanowire field-effect transistors. Journal of Semiconductors, 2009, 30(8): 084002

[4] Li Y G, Yang A C, Zhuo B S, et al. Growth of SiO_2 nanowires on different substrates using Au as a catalyst. Journal of Semiconductors, 2011, 32(2): 023002

[5] Eddy J C R, Gaskil D K. Silicon carbide as a platform for power electronics. Science, 2009, 324: 1398

[6] Marinella M J, Schroder D K, Chung G, et al. Carrier generation lifetimes in 4H-SiC MOS capacitors. IEEE Trans Electron Devices, 2010, 57: 1910

[7] Wu H, Sun G S, Yang T, et al. Effect of annealing process on the surface roughness in multiple Al implanted 4H-SiC. Journal of Semiconductors, 2011, 32(7): 072002

[8] Liu C J, Liu S, Feng J J, et al. Nickel ohmic contacts of high-concentration P-implanted 4H-SiC. Journal of Semiconductors, 2012, 33(3): 036002

[9] Seong H K, Choi H J, Lee S K, et al. Optical and electrical transport properties in silicon carbide nanowires. Appl Phys Lett, 2004, 85:1256

[10] Zhou W M, Fang F, Hou Z Y, et al. Field-effect transistor based on β-SiC nanowire. IEEE Electron Device Lett, 2006, 27: 463

[11] Rogdakis K, Bescond M, Bano E, et al. Theoretical comparison of 3C-SiC and Si nanowire FETs in ballistic and diffusive regimes. Nanotechnology, 2007, 18: 475715

[12] Rogdakis K, Lee S Y, Bescond M, et al. 3C-silicon carbide nanowire FET: an experimental and theoretical approach. IEEE Trans Electron Devices, 2008, 55: 1970

[13] Jang C O, Kim T H, Lee S Y, et al. Low-resistance ohmic contacts to SiC nanowires and their applications to field-effect transistors. Nanotechnology, 2008, 19: 345203

[14] Rogdakis K, Lee S Y, Kim D J, et al. Effect of source and drain contacts Schottky barrier on 3C-SiC nanowire FETs I–V characteristics. Mater Sci Forum, 2009, 615–617: 235

[15] Kang S J, Kocabas C, Ozel T, et al. High-performance electronics using dense, perfectly aligned arrays of single-walled carbon nanotubes. Nature Nanotech, 2007, 2: 230

[16] Cao Q, Rogers J A. Random Networks and aligned arrays of single-walled carbon nanotubes for electronic device applications. Nano Research, 2008, 1: 259

[17] Kocabas C, Kang S J, Ozel T, et al. Improved synthesis of aligned arrays of single-walled carbon nanotubes and their implementation in thin film type transistors. J Phys Chem C, 2007, 111: 17879

[18] Park W I, Zheng G F, Jiang X C, et al. Controlled synthesis of millimeter-long silicon nanowires with uniform electronic properties. Nano Lett, 2008, 8: 3004

[19] Wang F L, Zhang L Y, Zhang Y F. SiC nanowires synthesized by rapidly heating a mixture of SiO and arc-discharge plasma pretreated carbon black. Nanoscale Res Lett, 2009, 4: 153

[20] Motayed A, Vaudin M, Davydov A V, et al. Diameter dependent transport properties of gallium nitride nanowire field effect transistors. Appl Phys Lett, 2007, 90: 043104

[21] Ford A C, Ho J C, Chueh Y L, et al. Diameter-dependent electron mobility of InAs nanowires. Nano Lett, 2009, 9: 360

[22] Chen C X, Zhang W, Zhang Y F. Multichannel carbon nanotube field-effect transistors with compound channel layer. Appl Phys Lett, 2009, 95: 192110

[23] Duan X F, Niu C M, Sahi V, et al. High-performance thin-film transistors using semiconductor nanowires and nanoribbons. Nature, 2003, 425: 274

[24] Kumar S, Murthy J Y, Alam M A. Percolating conduction in finite nanotube networks. Phys Rev Lett, 2005, 95: 066802

[25] Whang D, Jin S, Wu Y, et al. Large-scale hierarchical organization of nanowire arrays for integrated nanosystems. Nano Lett, 2003, 3: 1255

[26] Huang Y, Duan X F, Wei Q Q, et al. Directed assembly of one-dimensional nanostructures into functional networks. Science, 2001, 291: 630

[27] Liu Y L, Chung J H , Liu W K, et al. Dielectrophoretic assembly of nanowires. J Phys Chem B, 2006, 110: 14098

[28] Vijayaraghavan A, Blatt S, Weissenberger D, et al. Ultra-large-scale directed assembly of single-walled carbon nanotube devices. Nano Lett, 2007, 7: 1556

[29] Fan D L, Cammarata R C, Chien C L. Precision transport and assembling of nanowires in suspension by electric fields. Appl Phys Lett, 2008, 92: 093115

[30] Raychaudhuri S, Dayeh S A, Wang D L, et al. Precise semiconductor nanowire placement through dielectrophoresis. Nano Lett, 2009, 9: 2260

[31] Freer E M, GrachevO, Duan X F, et al. High-yield self-limiting single-nanowire assembly with dielectrophoresis. Nature Nanotech, 2010, 5: 525

[32] Oh K, Chung J H, Riley J J, et al. Fluid flow-assisted dielectrophoretic assembly of nanowires. Langmuir, 2007, 23: 11932

[33] Chen C X , Yan L J, Kong E S W, et al. Ultrasonic nanowelding of carbon nanotubes to metal electrodes. Nanotechnology, 2006, 17: 2192

[34] Chen C X, Zhang Y F. Manipulation of single-wall carbon nanotubes into dispersively aligned arrays between metal electrodes. J Phys D: Appl Phys, 2006, 39: 172

[35] Chen C X, Xu D, Kong E S W, et al. Multichannel carbon-nanotube FETs and complementary logic gates with nanowelded contacts. IEEE Electron Device Lett, 2006, 27: 852

[36] Xu D D, Subramanian A, Dong L X, et al. Shaping nanoelectrodes for high-precision dielectrophoretic assembly of carbon nanotubes. EEE Trans Nanotechnol, 2009, 8: 449

[37] Kumara S, Rajaraman S, Gerhardt R A, et al. Tin oxide nanosensor fabrication using AC dielectrophoretic manipulation of nanobelts. Electrochim Acta, 2005, 51: 943

[38] Lao C S, Liu J, Gao P X, et al. ZnO nanobelt/nanowire Schottky diodes formed by dielectrophoresis alignment across Au electrodes. Nano Lett, 2006, 6: 263

[39] Smith P A, Nordquist C D, Jackson T N, et al. Electric-field assisted assembly and alignment of metallic nanowires. Appl Phys Lett, 2000, 77: 1339

[40] Lee S Y, Kim T H, Suh D I, et al. A study of dielectrophoretically aligned gallium nitride nanowires in metal electrodes and their

electrical properties. Chem Phys Lett, 2006, 427: 107
[41] Li J Q, Zhang Q, Peng N, et al. Manipulation of carbon nanotubes using AC dielectrophoresis. Appl Phys Lett, 2005, 86: 153116
[42] Hamers R J, Beck J D, Eriksson M A, et al. Electrically directed assembly and detection of nanowire bridges in aqueous media. Nanotechnology, 2006, 17: S280
[43] Xiao Z, Sharma H, Zhu M Y, et al. Dielectrophoresis-assisted deposition and alignment of single-walled carbon nanotubes for electronic-device fabrication. J Vac Sci Technol A, 2010, 28: 750
[44] Hulman M, Tajmar M. The dielectrophoretic attachment of nanotube fibers on tungsten needles. Nanotechnology, 2007, 18: 145504
[45] Zhou W M, Liu X, Zhang Y F. Simple approach to β-SiC nanowires: synthesis, optical, and electrical properties. Appl Phys Lett, 2006, 89: 223124
[46] Davydov S Y. Estimates of the spontaneous polarization and permittivities of AlN, GaN, InN, and SiC crystals. Phys Solid State, 2009, 51: 1231
[47] Powell J A, Matus L G, Kuczmarski M A. Growth and characterization of cubic SiC single-crystal films on Si. J Electrochem Soc, 1987, 34: 1558
[48] Lide D R. CRC handbook of chemistry and physics. Boca Raton: CRC Press, 2008
[49] Macfie G, Compton R G, Corti H R. Electrical conductivity and solubility of KF in N, N-Dimethylformamide up to 125 ℃. J Chem Eng Data, 2001, 46: 1300
[50] Sze S M, Ng K K. Physics of semiconductor devices. Hoboken: John Wiley & Sons Inc, 2006